Economic Geology, v. 77, pp. 745-754

ECONOMIC GEOLOGY

AND THE

BULLETIN OF THE SOCIETY OF ECONOMIC GEOLOGISTS

VOL. 77 JUNE–JULY, 1982 NO. 4

A SPECIAL ISSUE DEVOTED TO SKARN DEPOSITS

Introduction—Terminology, Classification, and Composition of Skarn Deposits

M. T. EINAUDI

Stanford University, Stanford, California 94305

AND D. M. BURT

Arizona State University, Tempe, Arizona 85281

SKARN deposits occur throughout a broad range of geologic environments from Precambrian to late Tertiary age. Most deposits of economic importance are relatively young, however, and are related to magmatic-hydrothermal activity associated with dioritic to granitic plutonism in orogenic belts. The feature that sets skarn deposits apart from other types of mineral deposits is the gangue—a coarse-grained, generally iron-rich, mixture of Ca-Mg-Fe-Al silicates, formed by metasomatic processes at relatively high temperature and termed skarn.

Since skarns are becoming increasingly important as sources of certain metals and as subjects for scientific investigation, the editors felt that a call for papers would result in a timely publication of data and ideas that could guide new or on-going exploration and research programs. Thus, the present issue of *Economic Geology* is devoted to papers dealing with the geology and geochemistry of skarn deposits, based on research being conducted in North America and Japan. The result is a major new descriptive and analytical data base for two dozen skarn deposits in Canada, the United States, Mexico, Japan, and Korea (Fig. 1, Table 1). Recent experimental studies on the stabilities of calc-silicates and a historical bibliography of skarn research round out the issue. Other topics that the editors planned to include, but which did not materialize, were reviews of metasomatic processes (e.g., Frantz and Mao, 1979; Walther and Helgeson, 1980), computational approaches to mass transport and water-rock reactions in carbonate environments (e.g., Norton et al., 1975), and light stable isotopes and fluid inclusions (e.g., Patterson et al., 1981). Some of these techniques are only now beginning to be applied to the study of skarn deposits—we hope that the present issue will provide an incentive for further studies.

The editors felt that they should begin this issue by introducing the reader to the terminology and classification of skarn deposits. The compositional variation of garnet and pyroxene is also discussed in the classification section; papers in the present issue add considerable detail to this subject, presenting over 700 electron microprobe analyses of garnets and pyroxenes from a large variety of ore types. In addition, the reader is referred to the "Historical Bibliography" (Burt, 1982) and to review papers by Burt (1972a and b, 1974, 1977), Shimazaki (1980), Einaudi et al. (1981), and Einaudi (1982).

Hornfels, Reaction Skarn, Skarnoid, and Skarn

Calc-silicate rocks associated with skarn deposits display a broad range of textures, compositions, and origins, because individual skarn deposits commonly are formed in complex, mixed host rocks, including carbonate, shale, volcanic, and plutonic rocks. At one end of the spectrum are calc-silicate hornfels, fine-grained and relatively homogeneous rocks formed by isochemical (except for devolatilization) metamorphic recrystallization of impure carbonates. The term hornfels has also been used in a descriptive sense for fine-grained metasomatically altered aluminous or siliceous rocks, such as those at Cantung (Dick and Hodgson, 1982). At the other end of the scale are the coarse-grained bodies of calc-silicate in relatively pure carbonates, formed by infiltration and diffusion of metasomatic fluids carrying exotic components, and referred to as skarn (also termed secondary skarn, replacement skarn, skarn proper, ore skarn, and tactite). Calc-silicate hornfels and skarn can be distinguished on the basis of geologic settings, morphology, grain size, and composition, and by the fact that skarns display metasomatic zoning. However, these recognition criteria are difficult to apply in cases involving interlayered shale or chert and limestone. In such cases, local exchange of components between the two rock types can occur, yielding reaction skarn (also referred to as local exchange skarn, bimetasomatic diffusion skarn, and calc-silicate bands). Like hornfelses, these are metamorphic rocks in that no intro-

0361-0128/82/34/745-10$2.50

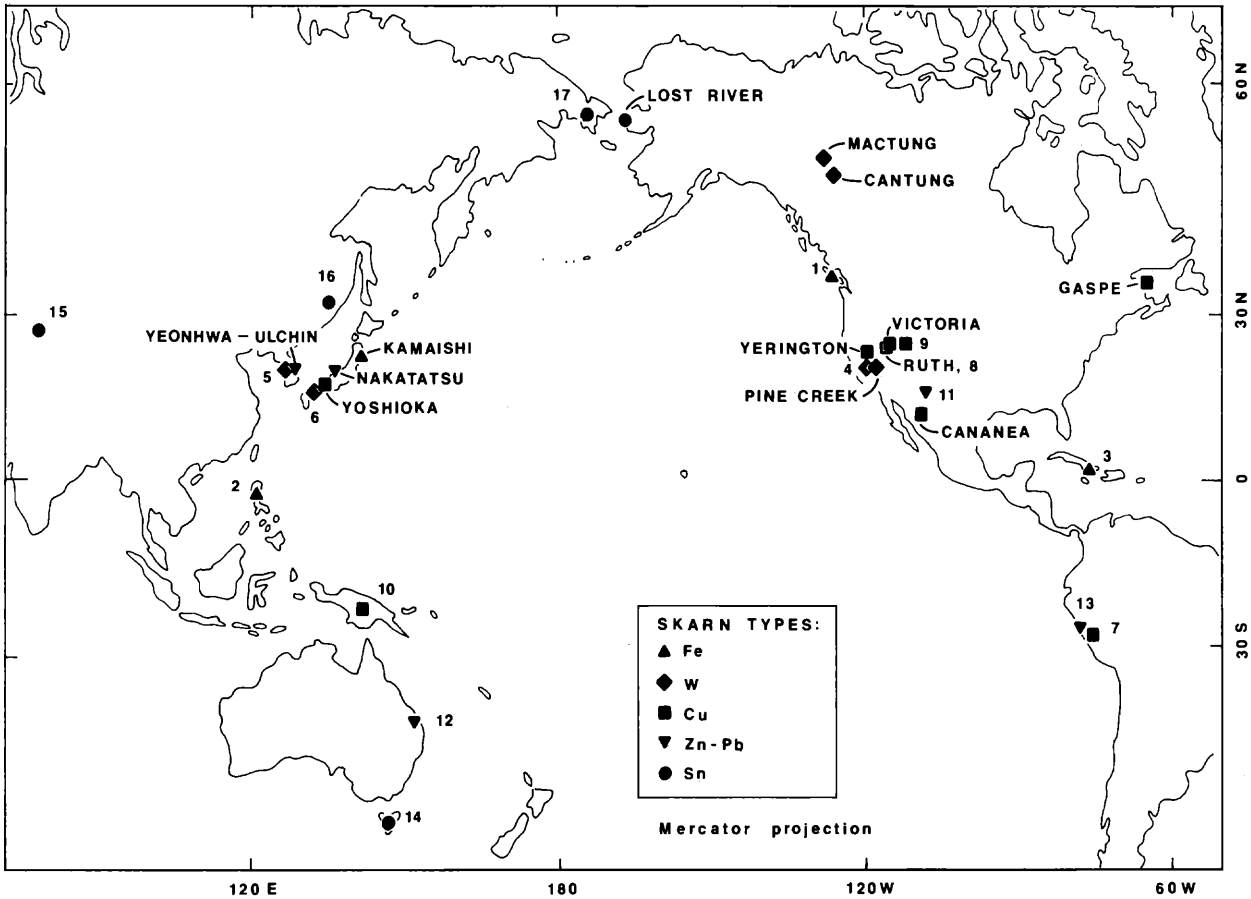

FIG. 1. Location of some skarn deposits described in this issue of *Economic Geology*, as well as additional examples (see Table 1).

duction of exotic components from outside the sedimentary section is required and, like skarns proper, they are metasomatically zoned. They can generally be distinguished from skarn by careful study of field relations and mineral compositions, but all gradations between reaction skarns and skarn are possible. This continuum is well illustrated by the descriptions of hornfels-marble contacts at Pine Creek (Newberry, 1982, figs. 6, 12, and 13) and Cantung (Dick and Hodgson, 1972, figs. 9, 26, and 28). Finally, the term skarnoid is used to refer to skarnlike rocks of uncertain or complex origin—often involving metasomatic alteration of impure carbonates, overprinting of skarn onto hornfels or reaction skarn, or large-scale homogenization of mixed lithologies (in effect, giant reaction skarns). A particularly striking example of skarnoid is described from the Yerington district (Harris and Einaudi, 1982).

Endoskarn

Skarns can be classified according to the rock type they replace. The terms exoskarn and endoskarn were originally applied to replacements of carbonates and intrusive rocks, respectively, in contact zones where the intrusive rock was presumed to be genetically related to the skarn-forming fluids. Some authors have advocated applying the term endoskarn to skarn formed in any aluminous rock, including shale and volcanic rocks, whereas others have applied the term silicate skarn to such metasomatic replacements.

The degree of development of endoskarn (sensu lato) and the relative volumes of endoskarn and exoskarn vary widely. Endoskarn is widespread in districts where metasomatic fluids utilized shale limestone, volcanic limestone, or dike limestone contacts as conduits, and where these were extensively fractured and therefore highly permeable. Such was the case for skarnoid in aluminous rocks and for endoskarn in granodiorite at Yerington, and to a lesser extent in hornfels at Mactung, and is a characteristic feature of Fe skarn deposits of the circum-Pacific andesitic terrains (e.g., Kamaishi; Uchida and Iiyama, 1982) and Zn-Pb skarn deposits formed along dikes (e.g., Yeonhwa-II; Yun and Einaudi, 1982). In deeper

TABLE 1. Classification of Calcic Skarn Deposits Described in this Volume as well as Additional Examples

	Iron	Tungsten	Copper	Zinc-lead	Tin-tungsten
Examples described in present volume	Shinyama deposit, Kamaishi mine, NE Japan	Pine Creek, California MacMillan Pass (Mactung), Yukon-N.W.T., Canada Canada Tungsten (Cantung), N.W.T., Canada	Sasano deposit Yoshioka mine, SW Japan Victoria mine, Nevada Douglas Hill and Casting Copper mines (Yerington district), Nevada Capote basin, Cananea district, Sonora, Mexico Ruth deposit, Robinson mining (Ely) district, Nevada Mines Gaspé, Quebec, Canada	Yeonhwa-I, Yeonhwa-II, and Ulchin mines, Taebaegsan, S. Korea Nakatatsu mine, central Japan	Lost River deposit, Alaska
Additional examples (numbers refer to localities on Fig. 1)	1. Empire mine, B.C., Canada (Sangster, 1969; Haug, 1976) 2. Larap, Camarines Norte, Philippines (Frost, 1965) 3. Daiquiri, Cuba (Lindgren and Ross, 1916)	4. Strawberry mine, California (Nokleberg, 1981) 5. Sangdong, Korea (John, 1963) 6. Fujigantani, SW Japan (Sato, 1980)	7. Morococha, Junín, Perú (Petersen, 1965) 8. Veteren, Tripp, and Liberty deposits, Robinson mining (Ely) district, Nevada (James, 1976) 9. Carr Fork mine, Bingham mining district, Utah (Atkinson and Einaudi, 1978) 10. Mt. Fubilan (Ok Tedi), Papua-New Guinea (Bamford, 1972)	11. Linchburg, New Mexico (Titley, 1961) 12. Ban Ban, Queensland, Australia (Ashley, 1980) 13. Uchucchacau, Cajatambo, Perú (Alpers, 1980)	14. Moina, Tasmania, Australia (Kwak and Askins, 1981) 15. Uchkoshkon, Kirgiziya SSR (Lisitsyn and Malinko, 1971) 16. Yaroslavsk, Primorsk, USSR (Materikov, 1977) 17. Itenyurginsk, Chukotka, USSR (Aleksandrov, 1974)

terrains, where plutons are less fractured and fluid circulation is more restricted, endoskarn forms only narrow zones at the immediate intrusive contact (e.g., Pine Creek). In cases where an endoskarn-exoskarn couplet is developed, ore generally is restricted to the exoskarn; however, where limestone is absent, endoskarns may contain ore (e.g., Yoshioka; Shimazaki, 1982). Finally, in cases where skarn develops near or over the tops of plutonic cupolas, as in most skarns related to porphyry copper plutons (e.g., Gaspé deposit, Allcock, 1982; Ruth deposit, Westra, 1982) and in tin skarns (e.g., Lost River; Dobson, 1982), endoskarn generally is absent. Endoskarn, therefore, is favored in those areas where fluid flow is dominantly into the pluton (presumably at depth) or upward along its contacts with carbonates, rather than where metasomatic fluid flow is dominantly up and out of the pluton. Infiltration, rather than diffusive exchange, is the major metasomatic process involved.

Endoskarns (sensu lato) display patterns of mineral zoning that dominantly reflect progressive addition of calcium to the protolith. Under relatively reducing conditions zoning toward limestone (or toward major fissures in the absence of limestone) consistently involves the sequence biotite → amphibole → pyroxene → (garnet). Any K-feldspar generally disappears with biotite, and plagioclase remains an important phase throughout except in the rare cases where garnet becomes dominant; the diagnostic assemblage is pyroxene-plagioclase. This sequence is typical of most W skarn and some Cu skarns, and is described in this issue for the diorite, quartz monzonite, and pelitic hornfels at Pine Creek, the pelitic hornfels at Mactung, and the black shale at Yoshioka. Under relatively oxidizing conditions, epidote-quartz is favored over pyroxene-plagioclase (Liou, 1973; Shimazaki, 1980) and garnet tends to be more abundant. Such cases are common in most Cu and Pb-Zn skarns and

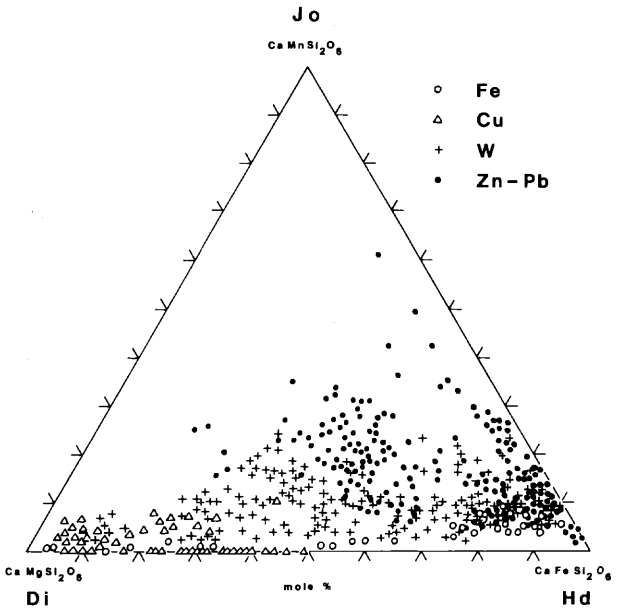

FIG. 2. Plot of electron microprobe analyses of pyroxenes from calcic skarn deposits classified by metal (Tables 1 and 2). Data from Haug (1976), Alpers (1980), Ashley (1980), Guy (1980), Sweeney (1980), Newberry (1980, 1982), Nockleberg (1981), Burton et al. (1982), Dick and Hodgson (1982), Harris and Einaudi (1982), Meinert (1982), Shimizu and Iiyama (1982), Uchida and Iiyama (1982), and Yun and Einaudi (1982).

are illustrated by the endoskarns in dolerite and slate at Nakatatsu (Shimizu and Iiyama, 1982) and in the quartz monzonite at Yeonhwa-II. An intermediate case is displayed by endoskarn in granodiorite at Yerington. The relative oxidation state of endoskarn is mirrored in the silicate and ore assemblages of exoskarns (see below).

Exoskarn

Classification of exoskarn can be made on the basis of dominant mineralogy, which in most cases reflects the composition of the carbonate rock replaced. Magnesian skarn contains an important component of Mg silicates, such as forsterite or its alteration product serpentine, commonly associated with diopside, calcite, and spinel. Although most magnesian skarns formed in dolomite, some, such as the Yerington skarns, formed after hydrothermal dolomitization of limestone. Except for a portion of the Yerington skarns, all deposits described in this issue are calcic skarns, containing an important component of Ca or Ca-Fe silicates such as garnet, pyroxenoids, or idocrase. Although most calcic skarns replace limestone, some, such as the skarn at the Mason Valley mine (Einaudi, 1977) and at Costabonne (Guy, 1980), replaced magnesian skarn. Thus, the modifiers magnesian and calcic should be used only in a descriptive sense; whether the source of major components in these skarns was the rock or the fluid may be determined only after detailed study; it will vary from deposit to deposit, and perhaps it will also vary with time in an individual deposit as a function of changing water rock ratios and compositional evolution of the skarn-forming fluid at its source.

Calcic Exoskarn

The bulk of the world's economic skarn deposits occurs in calcic exoskarns, and these are the major types described in this issue. Garnet and pyroxene are the dominant minerals in calcic exoskarn and represent the first products of water-rock reaction. Zoning during the early stages most commonly consists of garnet → pyroxene → (wollastonite) → marble. Many tin and tungsten skarns display an unusually high aluminum content, in which case idocrase occurs in addition to, or in place of, pyroxene or wollastonite (e.g., Pine Creek, Mactung, Lost River). Many Zn-Pb skarns are unusually Mn rich, in which case bustamite or rhodonite occurs in place of wollastonite (e.g., Nakatatsu, Yeonhwa-Ulchin).

The compositions of garnets and pyroxenes in calcic exoskarns are summarized in Figures 2 and 3, with the bulk of analyses taken from papers in the present issue. Pyroxenes display an increase in Mn

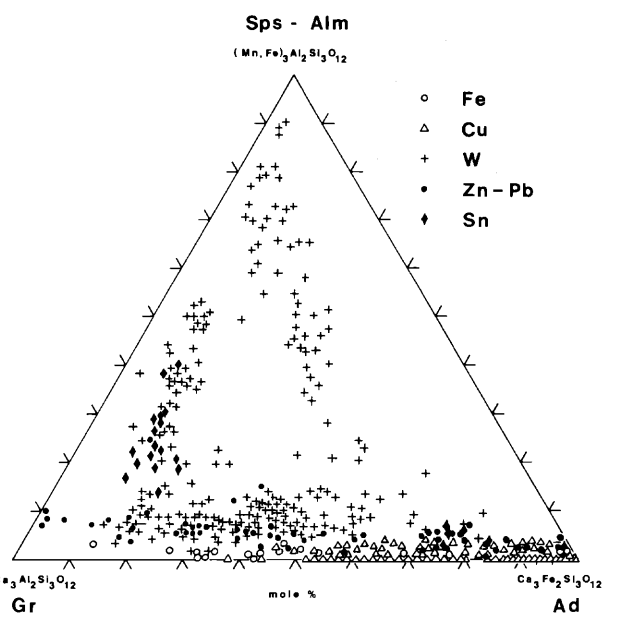

FIG. 3. Plot of electron microprobe analyses of garnets from calcic skarn deposits classified by metal (Tables 1 and 2). Data from Haug (1976), Ashley (1980), Guy (1980), Sweeney (1980), Newberry (1980, 1982), Nockleberg (1981), Burton et al. (1982), Dick and Hodgson (1982), Dobson (1982), Harris and Einaudi (1982), Meinert (1982), Shimizu and Iiyama (1982), Uchida and Iiyama (1982), and Yun and Einaudi (1982).

TABLE 2. Major Characteristics of the Five Classes of Calcic Skarn Deposits Listed in Table 1

	Iron	Tungsten (reduced)	Copper	Zinc-lead	Tin-tungsten
Typical size	5–200 m.t.	0.1–2 m.t.	1–100 m.t.	0.2–3 m.t.	0.1–3 m.t.
Typical grade	40% Fe	0.7% WO_3	1–2% Cu	9% Zn, 6% Pb, 5 oz/ton Ag	0.1–0.7% Sn
Metal associated	Fe, (Cu, Co, Au)	W, Mo, Cu, (Zn, Bi)	Cu, (Mo, Zn, W)	Zn, Pb, Ag, (Cu, W)	Sn, F, W, (Be, Zn)
Tectonic setting	Oceanic island arc; rifted continental margins	Continental margin, syn- to late orogenic	Continental margin, syn- to late orogenic	Continental margin, syn- to late orogenic	Continental; late to postorogenic or anorogenic
Associated igneous rocks	Gabbro to syenite; mostly diorite, some with diabase	Quartz diorite to quartz monzonite, rarely alaskite	Granodiorite to quartz monzonite	Plutons commonly absent; granodiorite to granite, diorite to syenite	Granite
Cogenetic volcanics in ore zone	Common; basalt; andesite	Absent	Rare; andesite, quartz latite	Absent	Absent
Pluton morphology	Large to small stocks, dikes	Large plutons, batholiths	Small stocks, dikes, breccia pipes	If present, stocks and dikes	Stocks, batholiths
Alteration in igneous rocks					
Endoskarn	Extensive in plutons, volcanics; epidote-pyroxene	Very local; pyroxene-plagioclase	Local; epidote-pyroxene-garnet	Local, but intense; epidote-pyroxene-garnet	Very rare
Other	Extensive Na silicates	Local quartz-biotite-muscovite-sulfide	Can be very extensive (e.g., prophyry Cu); biotite-orthoclase, quartz-sericite-pyrite	Local argillic, propylitic	Extensive greisen
Exsokarn composition	High in Fe; low in S, Mn	High in Al, Fe; low in S	High in Fe, S; low in Al, Mn	High in Fe, Mn, S; low in Al	High in Al, F; low in Fe, S
Early minerals	Ferrosalite (Hd_{20-80}), grandite (Ad_{20-95}), epidote, magnetite	Ferrosalite-hedenbergite (Hd_{60-90}, Jo_{5-20}), grandite (Ad_{10-50}), idocrase, wollastonite	Andradite (Ad_{60-100}), diopside (Hd_{5-50}), wollastonite	Manganoan hedenbergite (Hd_{30-90}, Jo_{10-40}), andraditic garnet (Ad_{20-100}, $spessartine_{2-10}$), bustamite, rhodonite	Idocrase, spessartine-rich grandite, Sn andradite, malayaite, danburite, datolite
Late minerals	Amphibole, chlorite, ilvaite	Spessartine $(_{5-35})$-almandine $(_{5-40})$-grandite, biotite, hornblende, plagioclase	Actinolite, (chlorite, montmorillonoids)	Mn actinolite, ilvaite, chlorite, dannemorite, rhodochrosite	Amphibole, mica, chlorite, tourmaline, fluorite
Ore minerals	Magnetite, (chalcopyrite, cobaltite, pyrrhotite)	Scheelite, molybdenite, chalcopyrite, (sphalerite, pyrrhotite, magnetite, pyrite, Bi°)	Chalcopyrite, pyrite hematite, magnetite, (bornite, pyrrhotite, molybdenite, tennantite)	Sphalerite, galena, pyrrhotite, pyrite, magnetite, (chalcopyrite, arsenopyrite)	Cassiterite, (scheelite, sphalerite, pyrrhotite, magnetite, pyrite, arsenopyrite.)

Notes: Based on Einaudi et al. (1981). Size expressed in millions of tons (m.t.). Range of garnet and pyroxene compositions (mole %) encompasses the most typical compositions of all studied examples. Garnet expressed as andradite (Ad), spessartine, and almandine—remainder is grossularite. Pyroxene expressed as hedenbergite (Hd) and johannsenite (Jo)—remainder is diopside. Ore minerals and metals in parentheses are relatively less abundant. Tungsten skarns summarized here are reduced types, as defined in Einaudi et al. (1981, table 6). Although magnetite is mined from many skarn types, the Fe skarns summarized here are those dominated by magnetite and occurring with mafic to intermediate plutonic and volcanic rocks (Einaudi et al., 1981, table 3)

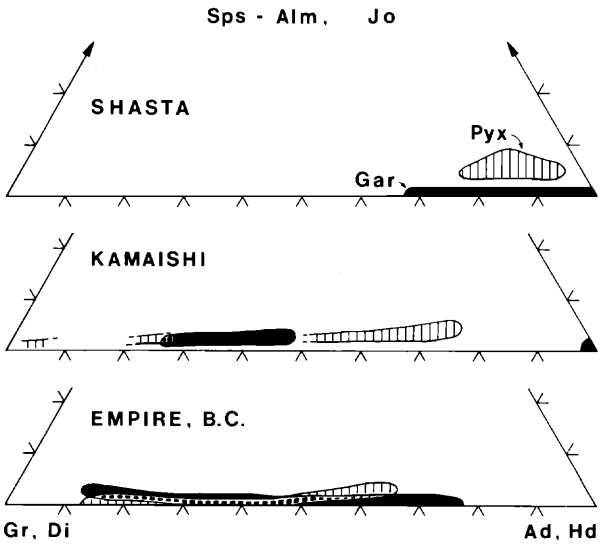

FIG. 4. Iron skarn deposits: compositional distribution of garnets (black) and pyroxenes (vertical ruling) plotted in terms of grossularite (Gr), andradite (Ad), and spessartine + almandine (Sps + Alm) and of diopside (Di), hedenbergite (Hd), and johannsenite (Jo). Data from Haug (1976), Uchida and Iiyama (1982), and Burton et al. (1982).

content with an increasing Fe/Mg ratio. This trend can be explained on the basis of the idealized substitutional order or preference (Burt, 1977) for cations in the M_1 structural site, based on mean M_{1-O} distance, which is Mg(2.077 Å) → Fe^{+2}(2.103 Å) → Mn(2.173 Å). A notable compositional gap is present (Fig. 2). It is defined by the maximum Mn content and extends from the diopside-johannsenite join well into ternary compositions; the absence of diopside-johannsenite solid solutions is presumably due to the unusual solution composition required, whereas the absence of pyroxenes near the johannsenite corner results in part from the instability of johannsenite relative to bustamite at skarn-forming temperatures (>400°C: Lamb et al., 1972; Albrecht and Peters, 1975) and in part from lack of analyses from the most Mn-enriched examples of Zn-Pb-Ag deposits (e.g., Simons and Munson, 1963).

Garnets (Fig. 3) display a broad range in composition, but the majority are grossular-andradite solid solutions containing less than 15 mole percent spessartine + almandine. Within this grandite area, the spessartine + almandine content increases with increasing substitution of Al for Fe^{+3} (increasing Gr/Ad). No skarn garnets plot on the grossular-andradite join at Gr/Ad > 70:30; this compositional area would be represented by metamorphic garnets in hornfelses and reaction skarns. Only tin and tungsten skarn deposits contain garnets with more than 20 mole percent spessartine + almandine and these have a Gr/Ad ratio greater than 35:65.

Classification of Skarn Deposits

Skarn deposits commonly are classified on the basis of the dominant economic metal. Fifteen deposits, representative of five major classes of calcic skarn deposits (Fe, W, Cu, Zn-Pb, Sn), are described in this issue. These, and additional representatives of each class, are listed in Table 1 and their geographic distribution is illustrated in Figure 1. A correlation of the metals contained with the tectonic setting and calc-silicate assemblages and compositions (Zharikov, 1970; Burt, 1972a; Shimazaki, 1980; Einaudi et al., 1981) is summarized in Table 2 and Figures 4 through 7. The sequence of descriptive papers in this issue reflects an idealized evolution of tectonic settings from island-arc diorite-andesite (Fe), to continental margin orogenic granodiorites and quartz monzonites (W, Cu, and Zn-Pb), to postorogenic or anorogenic granites (Sn-W).

A systematic relationship is seen between the composition of pyroxenes and garnets and the skarn type as defined in Table 2. An increase in hedenbergite and johannsenite and a decrease in diopside content of pyroxenes is exhibited through the deposit sequence Cu → Fe → W → Zn-Pb (Fig. 2), and an increase in grossular and spessartine + almandine and a decrease in andradite content of garnets is exhibited through the deposit sequence Cu → Fe → Zn-Pb → W (Fig. 3). Although skarns cannot be uniquely characterized by their garnet or pyroxene compositions alone, consideration of both yields a relatively unique fingerprint (Figs. 4 to 7) which serves as an additional aid in classification and in defining environments of formation.

Compositional variations of the type illustrated in Figures 4 to 7 can be cast in terms of the idealized end members grossularite + hedenbergite ("reduced" W skarns such as Mactung and Pine Creek) and andradite + diopside (Cu skarns), end members which largely reflect relatively reduced (sulfide-poor) and oxidized (sulfide-rich) conditions, respectively. Deviations from this scheme include the Mn enrichment of pyroxene in the Zn-Pb class (Yeonhwa-Ulchin, Nakatatsu), the iron-rich grandite-ferrosalite association of Fe skarns (Kamaishi), and the distinctive Fe^{+2}-Mn-enriched aluminous garnets that occur late in the development of W and Sn skarns (Mactung, Pine Creek, Lost River). Continuums within classes, i.e., from "reduced" tungsten (Mactung) to "oxidized" tungsten (Costabonne) (Fig. 5), as well as links between classes, i.e., between "oxidized" tungsten (Costabonne) and some sulfide skarns (e.g., Cananea, Fig. 6), are also present.

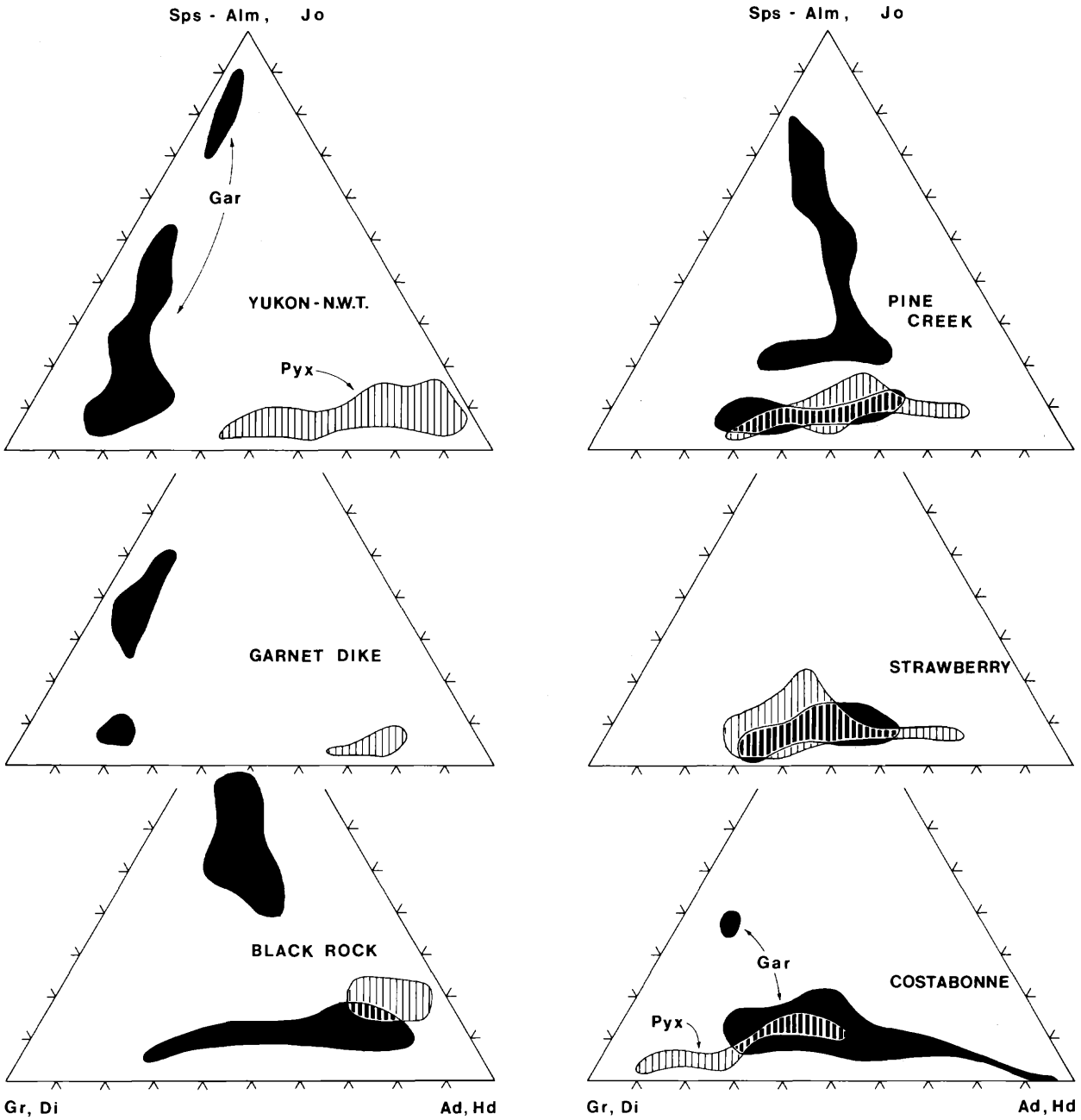

FIG. 5. Tungsten skarn deposits: compositional distribution of garnets (black) and pyroxenes (vertical ruling) plotted as in Figure 4. Data from Guy (1980), Newberry (1980, 1982), Nockleberg (1981), and Dick and Hodgson (1982).

Garnets and pyroxenes in most cases are not deposited simultaneously at equilibrium in one spot. Therefore, the compositional trends summarized above reflect a general skarn-forming environment and not a specific continuous reaction involving garnet, pyroxene, and additional phases. However, reactions such as hedenbergitic pyroxene + O_2 → andradite + quartz + magnetite serve to place limits on the skarn-forming environment, and Burt's (1972a) T-f_{O_2} grid for the system Ca-Fe-Si-C-O-H serves as a point of departure for such studies. Most skarns treated in this issue would require consideration of

the nine-component system Ca-Fe-Mg-Mn-Al-Si-C-O-H and its complex solid solutions over a temperature range of 600° to 200°C. Theoretical models for composition-activity relationships in minerals are being developed (e.g., Bird and Helgeson, 1980), but experimental verification is absent for most important skarn minerals. Papers in this issue dealing with the stability of hedenbergite-johannsenite (Burton et al., 1982) and hedenbergite-diopside (Gamble, 1982) solid solutions represent a first attempt at this problem and allow more accurate estimates of the oxidation-sulfidation states of skarns.

The oxidation-sulfidation state of skarn deposits must correlate with a combination of factors involving depth, reducing capacity of host rocks, and intrinsic oxidation state and acidity of magmas. As summarized by Einaudi et al. (1981), the reduced low sulfide skarns tend to be associated with the more reduced S-type or ilmenite series magmas and with I-type or magnetite series magmas of intermediate depth environments, whereas the oxidized, high sulfide skarns tend to be associated with the more oxidized I-type magmas of hypabyssal environments. An understanding of the causes of the systematic variations in metal content and calc-silicate compositions of skarn deposits must be tied to a firmer base of fluid inclusion studies to determine temperatures and chlorinities, and of light stable isotopes to understand the sources of water and water-rock ratios; such data, in conjunction with detailed field mapping and documentation of mineral abundance and compositions

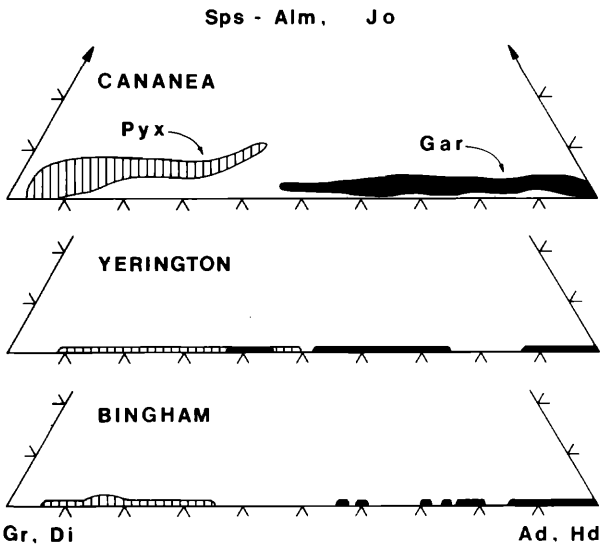

FIG. 6. Copper skarn deposits: compositional distribution of garnets (black) and pyroxenes (vertical ruling) plotted as in Figure 4. Data from Sweeney (1980), Meinert (1982), and Harris and Einaudi (1982).

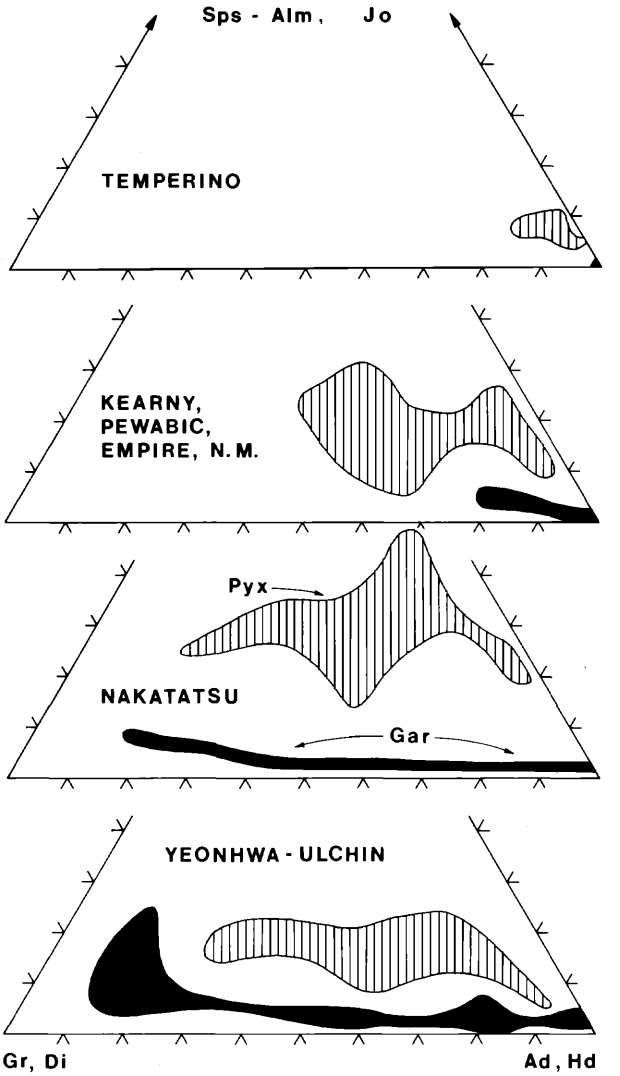

FIG. 7. Zinc-lead skarn deposits: compositional distribution of garnets (black) and pyroxenes (vertical ruling) plotted as in Figure 4. Data from Burton et al. (1982), Shimizu and Iiyama (1982), and Yun and Einaudi (1982).

for protolith and skarn, will ultimately yield a better understanding of the source and composition of the metasomatic fluid, of whether the fluid components are locally derived or introduced from outside the sedimentary section, and of the extent of wall-rock buffering of volatile fugacities. With such an understanding, the genetic relations between a given magma type and a given skarn type may begin to emerge.

Acknowledgments

The editors thank the many individuals who served as reviewers of the papers in this issue.

REFERENCES

Albrecht, J., and Peters, T., 1975, Hydrothermal synthesis of pyroxenoids in the system $MnSiO_3$-$CaSiO_3$ at pf = Z kb: Contr. Mineralogy Petrology, v. 50, p. 241–246.

Aleksandrov, S. M., 1974, Geochemistry of boron-tin mineralization in the magnesian skarns of eastern Chukotka: Geochemistry Internat., v. 11, p. 532–539.

Allcock, J. B., 1982, Skarn and porphyry copper mineralization at Mines Gaspé, Murdochville, Quebec: ECON. GEOL., v. 77, p. 971–999.

Alpers, C. N., 1980, Mineralogy, paragenesis, and zoning of the Luz vein, Uchucchacua, Perú: Unpub. B.A. thesis, Harvard Univ., 138 p.

Ashley, P. M., 1980, Geology of the Ban Ban zinc deposit, a sulfide-bearing skarn, southeast Queensland, Australia: ECON. GEOL., v. 75, p. 15–29.

Atkinson, W. W., Jr., and Einaudi, M. T., 1978, Skarn formation and mineralization in the contact aureole at Carr Fork, Bingham, Utah: ECON. GEOL., v. 73, p. 1326–1365.

Aktinson, W. W., Jr., Kaczmarowski, J. H., and Erickson, A. J., 1982, Geology of a skarn-breccia orebody at the Victoria mine, Elko County, Nevada: ECON. GEOL., v. 77, p. 899–918.

Bamford, R. W., 1972, The Mount Fubilan (Ok Tedi) porphyry copper deposit, Territory of Papua and New Guinea: ECON. GEOL., v. 67, p. 1019–1033.

Bird, D. K., and Helgeson, H. C., 1980, Chemical interaction of aqueous solutions with epidote-feldspar mineral assemblages in geologic systems. 1. Thermodynamic analysis of phase relations in the system CaO-FeO-Fe_2O_3-Al_2O_3-SiO_2-H_2O-CO_2: Am. Jour. Sci., v. 280, p. 907–941.

Burt, D. M., 1972a, Mineralogy and geochemistry of Ca-Fe-Si skarn deposits: Unpub. PhD thesis, Harvard Univ., 445 p.

—— 1972b, Silicate-sulfide equilibria in Ca-Fe-Si skarn deposits: Carnegie Inst. Washington Year Book 71, p. 450–457.

—— 1974, Metasomatic zoning in Ca-Fe-Si exoskarns: Carnegie Inst. Washington, Pub. 634, p. 287–293.

—— 1977, Mineralogy and petrology of skarn deposits: Soc. Italiana Mineralogia Petrologia Rend., v. 33, p. 859–873.

—— 1982, Skarn deposits—historical bibliography through 1970: ECON. GEOL., v. 77, p. 755–763.

Burton, J. C., Taylor, L. A., and Chou, I-M., 1982, The f_{O_2}-T and f_{S_2}-T stability relations of hedenbergite and hedenbergite-johannsenite solid solutions: ECON. GEOL., v. 77, p. 764–783.

Dick, L. A., and Hodgson, C. J., 1982, The Mactung W-Cu(-Zn) contact metasomatic and related deposits of the northeastern Canadian Cordillera: ECON. GEOL., v. 77, p. 845–867.

Dobson, D. C., 1982, Geology and alteration at the Lost River Sn-W-F deposit, Alaska: ECON. GEOL., v. 77, p. 1033–1052.

Einaudi, M. T., 1977, Petrogenesis of the copper-bearing skarn at the Mason Valley mine, Yerington district, Nevada: ECON. GEOL., v. 72, p. 769–795.

—— 1982, Skarns associated with porphyry copper plutons, I. Description of deposits, southwestern U. S., II. General features and origin, *in* Titley, S. R., ed., Advances in the geology of the porphyry copper deposits, southwestern United States: Tucson, Univ. Arizona Press, p. 139–183.

Einaudi, M. T., Meinert, L. D., and Newberry, R. J., 1981, Skarn deposits: ECON. GEOL., 75TH ANN. VOL., p. 317–391.

Frantz, J. D., and Mao, H. K., 1979, Bimetasomatism resulting from intergranular diffusion: II. Prediction of multimineralic zone sequences: Am. Jour. Sci., v. 279, p. 302–323.

Frost, J. E., 1965, Controls of ore deposition for the Larap mineral deposits, Camarines Norte, Philippines: Unpub. Ph.D. thesis, Stanford Univ., 173 p.

Gamble, R. P., 1982, An experimental study of sulfidation reactions involving andradite and hedenbergite: ECON. GEOL., v. 77, p. 784–797.

Guy, B., 1980, Étude géologique et pétrologique du gísement de Costabonne: Bur. Recherches Geol. Min. [Paris] Mem. 99, p. 237–250.

Harris, N. B., and Einaudi, M. T., 1982, Skarn deposits in the Yerington district, Nevada: Metasomatic skarn evolution near Ludwig: ECON. GEOL., v. 77, p. 877–898.

Haug, J. L., 1976, Geology of the Merry Widow and Kingfisher contact metasomatic skarn magnetite deposits, Northern Vancouver Island, British Columbia: Unpub. M.S. thesis, Univ. Calgary, 117 p.

Hochella, M. F., Jr., Liou, J. G., Keskinen, M. J., and Kim, H. S., 1982, Synthesis and stability relations of magnesium idocrase: ECON. GEOL., v. 77, p. 798–808.

James, L. P., 1976, Zoned alteration in limestone at porphyry copper deposits, Ely, Nevada: ECON. GEOL., v. 71, p. 488–512.

John, Y. W., 1963, Geology and origin of Sangdong tungsten mine, Republic of Korea: ECON. GEOL., v. 58, p. 1285–1300.

Kwak, T. A. P., and Askins, P. W., 1981, Geology and genesis of the F-Sn-W(-Be-Zn) skarn (wrigglite) at Moina, Tasmania, Australia: ECON. GEOL., v. 76, p. 439–467.

Lamb, C. L., Lindsley, D. H., and Grover, J. E., 1972, Johannsenite-bustamite: inversion and stability range [abs.]: Geol. Soc. America, Abstracts with Programs, v. 4, p. 571–572.

Lindgren, W., and Ross, C. P., 1916, The iron deposits of Daiquiri, Cuba: Am. Inst. Mining Engineers Trans., v. 53, p. 40–66.

Liou, J. G., 1973, Synthesis and stability relations of epidote, $Ca_2Al_2FeSi_3O_{12}(OH)$: Jour. Petrology, v. 14, p. 381–413.

Lisitsyn, A. Y., and Malinko, S. V., 1971, Physiochemical conditions for development of borosilicates and borates in limy skarn formation: Internat. Geology Rev., v. 13, p. 1773–1780.

Materikov, M. P., 1977, Deposits of tin, *in* Smirnov, V. I., ed., Ore deposits of the USSR: London, Pittman, v. 3, p. 229–294.

Meinert, L. D., 1982, Skarn, manto, and breccia pipe formation in sedimentary rocks of the Cananea mining district, Sonora, Mexico: ECON. GEOL., v. 77, p. 919–949.

Newberry, R. J., 1980, The geology and chemistry of skarn formation and tungsten deposition in the central Sierra Nevada, California: Unpub. Ph.D. thesis, Stanford Univ., 325 p.

—— 1982, Tungsten-bearing skarns of the Sierra Nevada, I: The Pine Creek mine, California: ECON. GEOL., v. 77, p. 823–844.

Nokleberg, W. J., 1981, Geologic setting, petrology and geochemistry of zoned tungsten-bearing skarns at the Strawberry mine, central Sierra Nevada, California: ECON. GEOL., v. 76, p. 111–133.

Norton, D., Titley, S. R., Gerlach, T., Knight, J. E., and Knapp, R. B., 1975, Hydrothermal systems notebook: Tucson, Univ. Arizona, Dept. Geosciences, p. V-1–V-12.

Patterson, D. J., Ohmoto, H., and Solomon, M., 1981, Geologic setting and genesis of cassiterite-sulfide mineralization at Renison Bell, western Tasmania: ECON. GEOL., v. 76, p. 393–438.

Petersen, U., 1965, Regional geology and major ore deposits of central Peru: ECON. GEOL., v. 60, p. 407–476.

Sangster, D. F., 1969, The contact metasomatic magnetite deposits of southwestern British Columbia: Canadian Geol. Survey Bull. 172, 85 p.

Sato, K., 1980, Tungsten skarn deposit of the Fujigatani mine, southwest Japan: ECON. GEOL., v. 75, p. 1066–1082.

Shimazaki, H., 1980, Characteristics of skarn deposits and related acid magmatism in Japan: ECON. GEOL., v. 75, p. 173–183.

—— 1982, The Sasano hastingsite-bearing copper skarn deposit formed in aluminous sediment at the Yoshioka mine, Japan: ECON. GEOL., v. 77, p. 868–876.

Shimizu, M., and Iiyama, J. T., 1982, Zinc-lead skarn deposits of

the Nakatatsu mine, central Japan: ECON. GEOL., v. 77, p. 1000–1012.

Simons, F. S., and Munson, E., 1963, Johannsenite from the Avavaipa mining district, Arizona: Am. Mineralogist, v. 48, p. 1154–1158.

Sweeney, M. J., 1980, Geochemistry of garnets from the North ore shoot, Bingham district, Utah: Unpub. M.S. thesis, Univ. Utah, 154 p.

Titley, S. R., 1961, Genesis and control of the Linchburg orebody, Socorro County, New Mexico: ECON. GEOL., v. 56, p. 695–722.

Uchida, E., and Iiyama, J. T., 1982, Physico-chemical study of skarn formation in the Shinyama iron-copper ore deposit of the Kamaishi mine, northeastern Japan: ECON. GEOL., v. 77, p. 809–822.

Walther, J. V., and Helgeson, H. C., 1980, Description and interpretation of metasomatic phase relations at high pressures and temperatures: I. Equilibrium activities of ionic species in non-ideal mixtures of CO_2 and H_2O: Am. Jour. Sci., v. 280, p. 575–606.

Westra, G., 1982, Alteration and mineralization in the Ruth porphyry copper deposit near Ely, Nevada: ECON. GEOL., v. 77, p. 950–970.

Yun, S., and Einaudi, M. T., 1982, Zinc-lead skarns of the Yeonhwa-Ulchin district, South Korea: ECON. GEOL., v. 77, p. 1013–1032.